

1
2
3
4
5
6
7
8
9
10
11
12
13
14

TITLE: Assessing giant sequoia mortality and regeneration following high severity wildfire

Authors: David N. Soderberg¹, Adrian J. Das¹, Nathan L. Stephenson¹, Marc D. Meyer², Christy A. Brigham³, and Joshua Flickinger³

¹U.S. Geological Survey, Western Ecological Research Center, Sequoia and Kings Canyon Field Station, Three Rivers, CA 93271, USA.

²USDA Forest Service, Southern Sierra Province Ecology Program, Bishop, CA 93514, USA.

³Sequoia and Kings Canyon national parks, Division of Resources Management and Science, Three Rivers, CA 93271, USA.

Corresponding author: David N. Soderberg (email: dsoderberg@usgs.gov).

Open Research: Data are not yet provided because they are currently under review as part of the USGS data release program. After acceptance of this manuscript by the journal and before publication, data will be archived in ScienceBase.

15 ABSTRACT

16 Fire is a critical driver of giant sequoia (*Sequoiadendron giganteum* [Lindl.] Buchholz)
17 regeneration. However, fire suppression combined with the effects of increased temperature and
18 severe drought have resulted in fires of an intensity and size outside of the historical norm. As a
19 result, recent mega-fires have killed a significant portion of the world's sequoia population (13 to
20 19%), and uncertainty surrounds whether severely affected groves will be able to recover
21 naturally, potentially leading to a loss of grove area. To assess the likelihood of natural recovery,
22 we collected spatially explicit data assessing mortality, crown condition, and regeneration within
23 four giant sequoia groves that were severely impacted by the SQF- (2020) and KNP-Complex
24 (2021) fires within Sequoia and Kings Canyon national parks. In total, we surveyed 5.9 ha for
25 seedlings and assessed the crown condition of 1140 trees. To inform management, we used a
26 statistical methodology that robustly quantifies the uncertainty in inherently 'noisy' seedling data
27 and takes advantage of readily available remote sensing metrics that would make our findings
28 applicable to other burned groves.

29 A loss of giant sequoia grove area would be a consequence of giant sequoia tree mortality
30 followed by a failure of natural regeneration. We found that areas that experienced high severity
31 fire (above ~800 RdNBR) are at substantial risk for loss of grove area, with tree mortality rapidly
32 increasing and giant sequoia seedling density simultaneously decreasing with fire severity. Such
33 high severity areas comprised 17.8, 142.0, 14.6, 1.6 hectares and ~90%, ~14%, ~53%, and ~27%
34 of Board Camp, Redwood Mountain, Suwanee, and New Oriole Lake groves, respectively. In all
35 sampling areas, we found that seedling densities fell far below the average density measured
36 after prescribed fires, where seedling numbers were almost certainly adequate to maintain giant
37 sequoia populations and postfire conditions were more in keeping with historical norms.

38 Importantly, spatial pattern is also important in assessing risk of grove loss, and in two groves,
39 Suwanee and New Oriole Lake, the high severity patches were not always contiguous,
40 potentially making some areas more resilient to regeneration failure due to the proximity of
41 surviving trees.

42 **Keywords:** giant sequoia, *Sequoiadendron giganteum*, high severity wildfire, tree mortality, fire
43 effects, natural regeneration, restoration management

44

45

INTRODUCTION

46
47
48
49
50
51
52
53
54
55
56
57
58
59
60
61
62
63
64
65
66
67
68

Throughout western North America, changes in land use patterns combined with the effects of severe drought – specifically, over a century of fire exclusion and large-scale tree mortality events – have led to shifts in forest structure and fire regimes throughout fire-prone forest ecosystems (Stevens et al., 2017, Parks & Abatzoglou, 2020, Hagmann et al., 2021). A resultant increase in ground and standing fuels, coupled with increasing temperatures and aridity, have facilitated an increase in wildfire-affected landscapes across the western United States (Westerling, 2016), with profound fire-induced changes within forest ecosystems of California (Safford et al., 2022).

In recent years, the southern Sierra Nevada mountains of California have been impacted by multiple fires of large extent that contained large patches that burned at high severity (Steel et al., 2022). Two of the largest recent fires within the southern Sierra Nevada, the SQF- fire of 2020 and the KNP-Complex fire of 2021 (hereafter referred to as the “SQF” and “KNP” fires) had cumulative burn areas of ~106,000 hectares, of which ~47,000 hectares were classified as ‘high severity’ (MTBS; www.mtbs.gov). While fire is an important and natural process in fire-adapted forest communities such as those in the Sierra Nevada (Stephens et al., 2007) – facilitating important ecosystem functions such as fuels reduction, landscape heterogeneity, and regeneration – large patches of high severity fire are not typical for mixed conifer forests and can lead to deleterious ecological outcomes, such as reduction of seed source, biodiversity, and wildfire and climate resilience (Cova et al., 2022). Large wildfires are not absent from the fire records of California forests, but the severity and scale of recent fire events have been outside the historical range of variation (Keeley & Sypard, 2021, Safford et al., 2022, Stephens et al., 2022). As such, these fires have had negative impacts on forest structure and ecosystem services,

69 including for species of special interest such as the giant sequoia (*Sequoiadendron giganteum*)
70 (Shive et al., 2022).

71 Giant sequoia has a limited distribution, covering ~11,000 hectares in ~70 groves across
72 the western slope of the Sierra Nevada (Stephenson & Brigham, 2021), much of which resides
73 within the boundaries of Sequoia National Park, CA (Hart, 2023). Due to their tremendous size,
74 longevity, and limited distribution, these charismatic macro-flora have inspired much public
75 admiration and been central to the designation of state parks, national monuments, and national
76 parks (Stephenson, 1996). Specifically, they were instrumental in the enabling legislation for
77 Sequoia and Kings Canyon national parks and are a focal resource in the parks' mission to
78 "...preserve unimpaired the natural and cultural resources and values of the national park
79 system..." (National Park Service Mission Statement).

80 Historically, southern Sierra Nevada wildfires tended to burn at low to moderate
81 severities, interspersed with small patches (<0.1 ha to a few hectares) of high-severity fire
82 (Stephenson et al., 1991, Stephenson, 1994, Stephenson, 1996), with a mean fire return interval
83 of ~15 years (Swetnam et al., 2009). Giant sequoia possesses a number of adaptations to fire,
84 including thick fire-resistant bark and semi-serotinous cones (Hartesveldt et al., 1975, Harvey et
85 al., 1980). Regeneration is abundant following fires, and especially within small gaps created by
86 local high severity fire, as the combination of exposed, friable mineral soil, canopy light
87 penetration, and seed release from semi-serotinous cones facilitates high levels of germination
88 (Hartesveldt et al., 1975, Harvey et al., 1980). Fire is a critical component for large-scale seed
89 release, with the heat pulse from a fire killing and opening cones (Hartesveldt et al., 1975,
90 Harvey et al., 1980). However, such seed release is predicated on episodic pulses of heat rather
91 than direct consumption of canopy and cones by fire. Such direct burning of the forest canopy

92 (crown fire) is a phenomenon that has been observed in high-severity burn areas within recent
93 catastrophic wildfires, and at the individual tree scale is referred to as ‘torching’. Indeed, post-
94 fire observations within large patches of recent high-severity wildfire (NPS communications)
95 suggest low levels of regeneration for giant sequoia that are potentially not commensurate with
96 grove reestablishment and resilience to future fire events. Generally, regeneration of giant
97 sequoia in large, high-severity patches is not yet well understood. Thus, given the high level of
98 mortality reported in Sierra Nevada giant sequoia groves within recent years (~13-19% of ‘large’
99 [>4 ft. diameter] giant sequoias; Stephenson & Brigham, 2021, Shive et al., 2022) – a situation
100 that is likely anomalous as giant sequoia is a fire-adapted species that can live for thousands of
101 years (Stephenson 2000, Sillett et al. 2015) and is in substantial contrast to more conservative
102 mortality estimates from previous prescribed burns, wildfires, and tree-ring records (Stephenson
103 1996) – there is uncertainty around whether large areas of high-severity fire impacted groves will
104 naturally regenerate to a state resembling their pre-fire structure (Figure 1).

105 Natural resources managers are currently tasked with deciding whether to replant areas of
106 groves where natural recovery without intervention is uncertain. To help inform this decision
107 making, we collected data on regeneration, tree mortality, and tree fire damage in four groves
108 recently affected by the SQF and KNP fires. Importantly, all these groves are candidates for
109 intervention. Our goal was to assess overall, postfire giant sequoia regeneration within our
110 sampled areas and to develop predictive models of regeneration as a function of neighborhood
111 metrics of scorched crown volume and a remotely sensed metric of fire burn severity -- RdNBR
112 (relativized differenced normalized burn ratio; Miller & Thode, 2007). We predicted that giant
113 sequoia regeneration would decline nonlinearly with high severity classified values of RdNBR,
114 corresponding with an increased percentage of giant sequoia crown torch (consumption by fire)

115 and decreased percentage of crown scorch (intact crown killed by heat) that would reduce the
116 available supply of viable giant sequoia seeds. This would result in some severely burned grove
117 areas with low probabilities of mean regeneration meeting critical thresholds of concern (i.e., low
118 probability of meeting seedling densities deemed adequate for successful natural regeneration).
119 Our models allowed us to use our mechanistic understanding of giant sequoia ecology and
120 regeneration to estimate seedling densities within large, contiguous high burn severity areas and
121 subsequently scale those predictions across high severity burn areas of recently fire-affected
122 groves.

123

124

METHODS

Study area

126 The California Sierra Nevada contains ~70 known giant sequoia groves, with ~40% of
127 giant sequoia grove area within the footprint of Sequoia and Kings Canyon (SEKI) National
128 Parks. In this study, we surveyed within four groves that experienced large areas of high severity
129 fire during the 2020 SQF (Board Camp grove) and 2021 KNP (Redwood Mountain, Suwanee,
130 and New Oriole Lake groves) wildfires (Figures 1,2).

131

Seedling sampling

133 To survey post-fire regeneration, we placed plots throughout the Board Camp, Suwanee,
134 and New Oriole Lake groves and within high severity burn regions of Redwood Mountain Grove
135 (areas with >75% basal area loss, Rapid Assessment of Vegetation Condition after Wildfire
136 (RAVG) 2022; <https://burnseverity.cr.usgs.gov/ravg/>) using the Generalized Random
137 Tessellation Stratified (GRTS) algorithm (Stevens & Olsen, 2004) with an equal probability

138 stratified sampling design (Figure 2). We used RAVG initial assessment (generally ≤ 45 days
139 after fire containment) data based on the relative differenced normalized burn ratio (RdNBR;
140 Miller & Thode, 2007) for the sampling design because extended assessment data (growing
141 season following the fire) was not available before sampling commenced. However, the two
142 metrics are largely consistent (Miller & Quayle, 2015). Plots in Redwood Mountain were limited
143 to high severity areas because the large size of the grove made a full sampling impractical and
144 high severity areas were of greater concern to resource managers based on previous studies of
145 postfire conifer regeneration in Sierra Nevada mixed conifer forests (Shive et al., 2018). We
146 surveyed plots in the 2021 SQF fire-affected Board Camp grove on April 27-28, 2022. We
147 surveyed the 2022 KNP fire-affected Redwood Mountain, Suwanee, and New Oriole Lake
148 groves within a 6-week span on Sept. 1-7, Sept. 25 – Oct. 5, and Oct. 12, 2022, respectively.
149 During field sampling, plot locations were found and recorded with a high-accuracy GPS device
150 (Javad Triumph-2, Eos Arrow Gold GNSS Receivers).

151 At each site, we tallied seedlings within fixed radius plots (Board Camp: 17.84m radius,
152 1/10thha, 20 plots; Redwood Mountain: 11.35m radius, $\sim 1/25^{\text{th}}$ ha, 45 plots, 17.84m radius,
153 1/10thha, 1 plot; Suwanee: 11.35m radius, $\sim 1/25^{\text{th}}$ ha, 30 plots; New Oriole Lake Grove: 11.35m
154 radius, $\sim 1/25^{\text{th}}$ ha, 20 plots; total sampled area: ~ 6 hectares). Generally, a plot radius of 11.35m
155 was used, with an increased radius of 17.84m used when seedling counts were sparse (i.e.,
156 entirety of Board Camp grove, when ≤ 2 seedlings were counted within initial 11.35m plot). Any
157 tree less than 1.37m in height was considered a seedling, though no seedlings in these surveys
158 exceeded 30cm tall. Given that (1) sequoias very rarely regenerate without fire (Harvey et al.,
159 1975, Shellhammer & Shellhammer, 2006), (2) severe fire likely killed all existing seedlings,
160 and (3) the small stature of all the seedlings counted, we were confident that all seedlings had

161 recruited postfire. In Board Camp, since sampling occurred two years after the fire, existing
162 seedlings could have established in the first year after fire (first cohort seedlings) or in the second
163 year after fire (second cohort seedlings). At Board Camp, we distinguished between cohorts
164 based on the presence of cotyledon leaves, which can still be found on seedlings for some time
165 after establishment. Based on the lack of cotyledon leaves on any Board Camp seedlings we
166 observed, we found no evidence of second cohort seedlings in the Board Camp grove despite a
167 robust sampling effort.

168

169 *Tree mortality and crown damage sampling*

170 We took advantage of an existing spatially explicit giant sequoia stem map (Sequoia Tree
171 Inventory 1973; ‘STI’) with individual tree attribute data (e.g., diameter at breast height) to
172 assess post-fire giant sequoia tree damage and mortality. We conducted a full survey of all
173 mapped giant sequoia trees within Board Camp, Suwanee, and New Oriole Lake groves. In
174 contrast, within the large Redwood Mountain grove, tree mortality and damage data were
175 recorded only for giant sequoias within 50m of study plot centers. For each tree in the survey, we
176 recorded the tree status (live/dead) and % of its crown that was live, scorched, or torched. We
177 defined foliage as ‘live’ if green, ‘scorched’ if dead and brown (presumably killed from fire heat
178 pulse), and ‘torched’ if foliage was blackened from fire char or missing (e.g., blackened, bare
179 branches) but presumably consumed during the SQF or KNP fires.

180 We estimated crown volumes (m^3) for each giant sequoia in our dataset using diameter
181 values from STI and an allometric equation relating tree diameter to crown volume (m^3) (Sillett
182 et al., 2019, see Appendix S1: Figure S1). To calculate crown volume of live, scorched, and
183 torched foliage, we multiplied the estimated individual tree crown volumes by the recorded

184 proportion of crown that was live, scorched, or torched. To calculate ‘neighborhood’ crown
185 volumes of live, scorched, or torched canopies, respectively, we summed all tree crown volume
186 estimates for all giant sequoia within the 50-meter radius ‘neighborhood’ (wherein a majority of
187 the seed rain contribution from a large giant sequoia will fall, see Clark et al., 2021), of a study
188 plot centroid.

189

190 *Fire Perimeters and Burn Severity*

191 Burn area boundary polygons and spatially explicit severity raster data (e.g., RdNBR
192 values) for the SQF and KNP fires were sourced from Monitoring Trends in Burn Severity
193 (MTBS; www.mtbs.gov). MTBS raster datasets are generated from Landsat (TM/EMT+/OLI)
194 image data which is acquired at a spatial resolution of 30 meters. MTBS vector datasets (burn
195 scar boundaries) are delineated from imagery and burn severity index data at a map scale of
196 1:24,000 to 1:50,000. Within Board Camp, Suwanee, and New Oriole Lake groves, our plots fell
197 within high severity patches roughly in proportion to the total high severity area in the given
198 grove (high severity: BOCA - ~92% area, 90% plots; SUWA - ~40% area, 37% plots; NEOL -
199 ~46% area, 50% plots). As noted above, our study locations within Redwood Mountain grove
200 were specifically chosen within high severity burn areas (high severity ~28% area, 100% plots).

201

202 *Statistical Analysis*

203 To estimate the seedling densities (SDens) at each surveyed giant sequoia grove, we fit
204 an intercept-only negative binomial count model (Eq.2 without parameters). This is conceptually
205 equivalent to a simple average, although using a negative binomial distribution to determine the
206 density is more appropriate for count data and our Bayesian methodology also allowed us to

207 directly describe the uncertainty in our estimate as a probability distribution (Figure 3, Table 1),
208 where the quantifiable uncertainty can be used to calculate the probability of the true mean being
209 above or below specified values (see Tables 1,2).

210 To assess the spatial relationship between ground measurements and a remote-sensed
211 measure of burn severity, we applied a negative binomial generalized additive model (GAM) to
212 estimate seedlings densities as a function of the burn severity metric ‘RdNBR’ (see Miller &
213 Thode, 2007) (Eq. 2). As seedling densities are considerably influenced by mortality rates over
214 time, we fit a separate model for data from groves affected by the 2020 SQF (i.e., Board Camp
215 grove) and the 2021 KNP fires (i.e., Redwood Mountain, Suwanee, and New Oriole Lake
216 groves) (Figure 4).

217 To assess the relationship between our ground-based measurements of giant sequoia
218 crown conditions, we used negative binomial generalized linear models (GLM) to assess the
219 relationship between seedling density and ‘neighborhood’ crown volumes of live (CVL),
220 scorched (CVS), and torched (CVT) foliage (aggregate live, scorched, and torched crown
221 volumes within a 50m radius of plot center) as a function of RdNBR (Eq. 2, Figure 5). Crown
222 volumes of individual giant sequoias were calculated using an allometric equation derived from
223 Sillett et al., (2016) (Eq. S1, Figure S1), with individual crown volumes of live, torched, and
224 scorched foliage proportionally allocated based on our field measurements.

225 Additionally, given our mechanistic assumptions of giant sequoia cone semi-serotiny and
226 observed relationship between regeneration and heat pulse induced crown scorch (i.e., ‘CVS’,
227 see Harvey et al., 1980), we assessed the relationship between neighborhood crown volume
228 scorch and RdNBR to bridge the mechanistic rationale underpinning an association between
229 seedling density and RdNBR using the same GLM approach described above (Eq. 3 Figure S2).

230 Our models are structured with normal prior distributions and are described as follows:

$$231 \quad y_i \sim \text{NB}(m, q) \quad (1)$$

232 where y_i is the seedling count for the i th observation and m and q are the mean and the
233 shape parameter of the negative binomial distribution, respectively. The mean parameters are
234 related to the variables X_i (i.e., $SDens$, CVL , CVS , CVT , $RdNBR$) for i th observations via the
235 following link function:

$$236 \quad \log(m_i) = \alpha + \log(T_i) + (X_i)\beta + e_i \quad (2)$$

$$237 \quad CVS_i = \alpha + (RdNBR_i)\beta + e_i \quad (3)$$

238 where $\log(T_i)$ is an ‘offset’, which corrects for the variation in surveyed area amongst i th
239 observations, α is the intercept, β is the parameter estimate, and e_i is the residual error associated
240 with the i th observation.

241 The model parameters were drawn from normal distributions centered around the mean
242 and estimated variances of our data. Specifically:

$$243 \quad \mu SDens_i \sim \text{Normal}(\mu SDens, SDens\sigma^2) \quad (4)$$

$$244 \quad \mu CVL_i \sim \text{Normal}(\mu CVL, CVL\sigma^2) \quad (5)$$

$$245 \quad \mu CVS_i \sim \text{Normal}(\mu CVT, CVT\sigma^2) \quad (6)$$

$$246 \quad \mu CVT_i \sim \text{Normal}(\mu CVS, CVS\sigma^2) \quad (7)$$

$$247 \quad \mu RdNBR_i \sim \text{Normal}(\mu RdNBR, RdNBR\sigma^2) \quad (8)$$

248 The model parameters were given normal, diffuse priors with wide distributions.

249 Specifically:

$$250 \quad \mu SDens, \mu CVL, \mu CVS, \mu CVT, \mu RdNBR \sim \text{Normal}(0, 1000) \quad (9)$$

251 With the exception of the variance parameters, which were given a modest, Student-t
252 prior distribution: Specifically:

253 $SDens\sigma^2, CVL\sigma^2, CVS\sigma^2, CVT\sigma^2, RdNBR\sigma^2 \sim \text{Student-t}(0,3)$ (10)

254 We conducted all analyses in R version 4.3.2 (R Core Team 2022) by computing
255 Bayesian parameter estimates via Markov chain Monte Carlo (MCMC) sampling. Statistical
256 package “rstanarm” (Goodrich et al., 2022, Stan Development Team 2023) was used to compute
257 4 MCMC chains for 2,000 iterations, discarding the first 1,000 iterations as burn-in and sampling
258 each iteration thereafter. All models were checked graphically for convergence and Rhat (\hat{r})
259 values (i.e., the Gelman–Rubin convergence diagnostic (Gelman & Rubin, 1992)), a ratio of
260 variation within and between MCMC chains, were less than 1.01, indicating thorough MCMC
261 sampling and convergence of the posterior distributions.

262 Using Bayesian MCMC estimates, a median estimate and quantified uncertainty were
263 derived for each model parameter. The median estimate (ME) and 90% Bayesian credible
264 intervals were then calculated as the median model parameter, bounded by the range of values
265 indicating the equal-tail 90% credible interval of the true parameter estimate. The marginal
266 probability (MP) is the probability that the mean estimate of a parameter (e.g., slope coefficient
267 for the relationship between a response and predictor variable) is statistically different (greater or
268 less than) than zero. MP was estimated by calculating the total number of parameter MCMC
269 estimates greater (or less) than the test comparison (e.g., ‘0’), divided by the total number of
270 MCMC estimates. To provide a reference for managers, we also used MP to compare seedling
271 densities estimated in this study with those estimated from seedling data collected after
272 prescribed fires (Stephenson et al., in prep).

273

274 RESULTS

275 *Seedling Overview*

276 Our seedling surveys covered ~10.0%, ~4.3%, and ~5.5% of the total area in Board
277 Camp, Suwanee, and New Oriole Lake groves, respectively. Within the much larger Redwood
278 Mountain grove, ~1.5% of the high burn severity area was surveyed. Within the 20 plots in the
279 SQF (2020) fire affected Board Camp grove, we counted 3221 seedlings across ~2.0 ha of
280 census area. None of the seedlings were identified as second cohort (germinated the second year
281 following fire), strongly suggesting very little additional regeneration in the second year after the
282 fire. Within the 46 plots in Redwood Mountain grove, we counted 19282 seedlings across ~1.9
283 ha of the ~350ha of high severity burn area. Within the 30 plots in Suwanee grove, we counted
284 14239 seedlings across ~1.2 ha. Within the 20 plots in New Oriole Lake grove, we counted
285 13025 seedlings across ~0.8 ha (Table 1). In general, seedling surveys within the KNP (2021)
286 affected Redwood Mountain, Suwanee, and New Oriole Lake groves yielded substantially higher
287 numbers than those at Board Camp, as expected given that Board Camp only had first cohort
288 seedlings that had experienced at least an additional 6 months of exposure to mortality.

289

290 *Estimating overall seedling densities*

291 To provide conservative comparisons, we contrast second cohort reference densities
292 presented in Stephenson et al., (in prep) with giant sequoia seedling densities measured within
293 Board Camp, high burn severity portions of Redwood Mountain, Suwanee, and New Oriole Lake
294 groves. For the SQF (2020) affected Board Camp grove, the modeled median of the probability
295 distribution for seedling density was 1609 with a 90% credible interval (CI) of 1749 to 4709
296 seedlings/ha. For comparison, the estimated mean seedling density in the first year after
297 prescribed fire (Stephenson et al., in prep) was 173742 (90% CI: 73468 – 605985) seedlings/ha
298 with median second cohort seedling densities of 39562 (90% CI: 16357 – 133134) seedlings/ha.

299 We found the marginal probability of Board Camp seedling densities being equivalent to those
300 the second year after prescribed fire was <0.1%.

301 For the KNP (2021) affected high burn severity area of Redwood Mountain, the modeled
302 median of the probability distribution for seedling density was 10541 (90% CI: 7412 – 15678
303 seedlings/ha), with a marginal probability of Redwood Mountain seedling densities being
304 equivalent to those the second year after prescribed fire of 1.1%. Within Suwanee grove, the
305 median of the probability distribution for seedling density was 11769 (90% CI: 7487 – 20000
306 seedlings/ha), with a marginal probability of Suwanee seedling densities being equivalent to
307 those the second year after prescribed fire of 2.4%. Within New Oriole Lake grove, the median
308 of the probability distribution for seedling density was 16988 (90% CI: 9595 – 35181
309 seedlings/ha), with a marginal probability of New Oriole Lake seedling densities being
310 equivalent to densities the second year after prescribed fire of 11.2%.

311

312 *Estimating local seedling densities*

313 We found that seedling densities increased with increasing volume of ‘neighborhood’
314 crown scorch. The relationship was ‘noisy’ (see Appendix S1: Figure S2), but, for both fires,
315 marginal probabilities strongly suggest the relationship is real (100% and 93.8% marginal
316 probability of the parameter being greater than 0 for the SQF and KNP fires, respectively). This
317 result is consistent with scorched giant sequoia crowns having intact, heat-killed cones that
318 release abundant viable seed, thus yielding higher local seedling densities (see Introduction and
319 Discussion). We also found that across groves the volume of scorched foliage decreased (97.8%
320 marginal probability of being <0) and the volume of torched foliage increased (99.9% marginal
321 probability of being >0) with increasing RdNBR (Figure 5), indicating that RdNBR was

322 sensitive to an increasing percentage of torched foliage (i.e., as fire severity increased more of
323 the crown was directly consumed by fire, leaving less scorched foliage and cones).

324 Not surprisingly, we also found a strong relationship between seedling density and
325 RdNBR in both the SQF (2020) affected Board Camp and KNP (2021) affected Redwood
326 Mountain, Suwanee, and New Oriole Lake groves (Figure 4), with seedling densities and the
327 variability in seedling densities decreasing with increasing RdNBR. In general, across our
328 sampled range, the probability of seedling densities reaching the average levels seen the second
329 year after prescribed fires is very low, with the occurrence of any plots with relatively high
330 seedling densities dropping noticeably for RdNBR values above 800 in Board Camp and above
331 1100 in the other groves (Figure 4, Table 2). For our fitted seedling density to RdNBR
332 relationship within Board Camp grove, we excluded one outlier plot that had a very high density
333 of seedlings in an area with a relatively low volume of local crown scorch and a relatively high
334 value of RdNBR. This outlier, and high degree of data variance or ‘noise’, generally suggests
335 additional mechanisms beyond local crown scorch that can affect seedling occurrence (see
336 Discussion), but our data indicate that such mechanisms, while almost certainly causing an
337 increase in variability, rarely result in high seedling densities in areas of very high severity fire
338 (Figure 4).

339

340 *Grove-level tree mortality*

341 We completed a full survey of tree mortality and crown fire damage at Board Camp,
342 Suwanee, and New Oriole Lake groves, and within 50m of each study plot center in Redwood
343 Mountain grove. Tree mortality was 81.0% (230/284), 43.6% (144/330), and 43.1% (28/65
344 within the entire grove areas of Board Camp, Suwanee, and New Oriole Lake groves,

345 respectively. However, within the high burn severity portions of each grove (>640 RdNBR, see
346 Miller & Thode, 2007), tree mortality rates were much higher – 91.4% (169/185), 60.6% (60/99),
347 76.7% (23/30), and 90.5% (417/461) of Board Camp, Suwanee, New Oriole Lake, and Redwood
348 Mountain groves. We found a very strong relationship between RdNBR and tree mortality
349 (Figure 5), and, as expected, mortality was high across the high severity zones. Specifically,
350 across all groves the majority of sampled plots within areas of ~800 or greater RdNBR had 0
351 surviving sequoias and/or the ‘neighborhood’ volume of live foliage dropped precipitously to
352 near 0 (e.g., a single live ‘neighborhood’ giant sequoia with 10% remaining live foliage) (Figure
353 5). This relationship, combined with the negative relationship between RdNBR and seedling
354 density, allows us to produce a RdNBR-based heat-map (Figure 6) indicating areas with a high
355 probability of both complete tree mortality and low levels of regeneration (Figures 4,5).

356

357

DISCUSSION

358

359

360

361

362

363

364

365

366

367

A permanent or long-term loss of giant sequoia grove area would be a consequence of
giant sequoia tree mortality followed by a failure of natural regeneration. In that context, our
results suggest that areas that experienced high severity fire in both the SQF-affected Board
Camp grove and KNP-affected Redwood Mountain, Suwanee, and New Oriole Lake groves
appear to be at substantial risk for loss of grove area. Mortality was very high in the high burn
severity patches in all groves sampled, and high severity areas comprise 17.8 hectares and ~90%
of the grove area in Board Camp and 142.0, 14.6, 1.6 hectares and ~13.5%, 52.7%, and ~27.0%
of Redwood Mountain, Suwanee, and New Oriole Lake groves, respectively. Furthermore, our
data (sampled grove-wide at Board Camp, Suwanee, and New Oriole Lake, and in high severity
areas in Redwood Mountain) indicate that overall seedling densities likely fall far below those

368 typically seen the second year after prescribed fire (Table 1 and Stephenson et al., in prep),
369 where regeneration was almost certainly adequate to maintain giant sequoia populations (York et
370 al., 2013) and postfire conditions were more in keeping with historical norms (Stephenson 1996).

371 More in-depth analyses suggest risk of regeneration failure increased with increasing fire
372 severity, likely as a function of reduced seed availability due to direct consumption of cones
373 during the fire. In Board Camp grove, mortality and high probability of regeneration failure
374 covered much of the northern and eastern part of the grove (Figure 6). For Redwood Mountain,
375 areas at highest risk for grove loss occurred mostly in the southern part of the grove. Within
376 Suwanee and New Oriole Lake groves, inadequate natural regeneration and loss of parent seed
377 trees was not as severe, comparatively, but still showed a substantial risk of some grove area loss
378 in several portions of Suwanee and the northern and southern extents of New Oriole Lake
379 (Figure 6). Importantly, the pattern of tree mortality in Suwanee, and to a lesser extent New
380 Oriole Lake, was less contiguous—often leaving some live and mature giant sequoia trees in or
381 near high severity patches. In such cases, regeneration failure should be less likely to lead to
382 permanent loss of grove area, as existing seed trees remain as a source of replenishment after
383 future fires – so long as those fires are in keeping with the heterogeneous, mixed-severity fire
384 regimes within which giant sequoias evolved.

385 As is common with regeneration data, there is considerable variability or ‘noise’ in the
386 dataset. This argues strongly for robust data collection (e.g., we collectively surveyed nearly 6 ha
387 of territory using a robust spatial sampling design) and use of statistical methods well-suited for
388 characterizing uncertainties in an easily interpretable manner. For example, Figures 3, 4, and 5
389 illustrate how data depth and inherent variability affect the confidence in our estimates.

390 Nevertheless, it is clear that natural regeneration is very unlikely to reach historical numbers in
391 any of the sampled areas.

392

393 *Mechanisms*

394 We hypothesized, based on previous research, that seedling densities would in part be a
395 function of the availability of seeds from giant sequoia cones killed by a heat pulse into the
396 crown, as such cones are known to be an important source of seed release postfire (Stark, 1968,
397 Hartesveldt et al., 1975, Harvey et al., 1980). Due to the great height of giant sequoia tree
398 canopies, there was no practical way to count cones directly. We therefore further hypothesized
399 that scorched foliage—foliage killed by a heat pulse into the crown—should be associated with
400 heat-killed cones, and therefore, subsequent seedling densities. Though the relationships have
401 substantial inherent variability, our results were generally consistent with this hypothesis (Figure
402 4, Appendix 1: Figure S2), with our remote sensing analysis providing further support (see
403 below).

404 The noise in the scorch-seedling density relationship is likely the result of a variety of
405 factors, including tree-to-tree variation in cone crops among sequoias, as well as inherent error in
406 our dbh-based crown volume allometry and in visual estimations of crown conditions from
407 ground observations. This may explain why the relationship between RdNBR and seedling
408 density (Figure 4) was less noisy than relationships derived from ground-based measures
409 (Appendix 1: Figure S2). In addition, our approach assumed crown scorch volume was linearly
410 related to heat-killed cones, an assumption that may not hold in practice, and our method would
411 also not capture tree-to-tree variability in cone load, which can be substantial (Sillett et al.,
412 2019). Finally, and perhaps most importantly, there are additional ecological ‘filters’ between

413 seed fall and seedling establishment—with a variety of factors that might weaken the
414 relationship between local seed production and local seedling establishment (see ‘*Uncaptured*
415 *Mechanisms*’).

416

417 *Extrapolating within and across groves using remote sensing*

418 Our analysis supports the hypothesis that greater scorched crown volume results in
419 increased seed rain, and therefore, higher seedling densities (Appendix 1: Figure S2). In addition,
420 our results show that, within high severity areas ($RdNBR > 640$), RdNBR values reflect the level
421 of crown scorch and torch (Figure 5). As noted above, the relationships between RdNBR and
422 seedling density were in fact less noisy than those developed using ground-based measures
423 (Figure 4, Appendix 1: Figure S2). Since the majority of our data were collected in areas
424 classified as having experienced high severity fire (i.e., most if not all of the standing trees were
425 killed in the fire), relatively lower RdNBR values in the context of our samples meant that dead
426 trees had retained more scorched foliage while higher RdNBR values indicated that an increasing
427 percentage of the crowns, and therefore cones, had been torched (i.e., consumed directly by fire).

428 In short, our results indicate that RdNBR can be used to estimate seedling density within
429 high severity areas of Board Camp, Redwood Mountain, Suwanee, and New Oriole Lake groves.
430 Similarly, RdNBR was highly effective at detecting adult giant sequoia mortality (Figure 5)
431 within all sampled groves. Given that RdNBR is a standardized measure used across fires, one
432 would expect these relationships to be effective across other burned groves. This suggests
433 RdNBR—taken as a continuous variable rather than by broad fire severity categories—is a
434 powerful tool for assessing the adequacy of sequoia regeneration in any giant sequoia grove after
435 a wildfire.

436 Using RdNBR to estimate giant sequoia regeneration densities does have limitations.
437 RdNBR values can be influenced by shadows, clouds, and other atmospheric disturbances (Hoy
438 et al., 2008, Verbyla et al., 2008, Fassnacht et al., 2021). Also, as RdNBR does not distinguish
439 between giant sequoias and other canopy vegetation, spectral changes in other parts of the
440 canopy and/or understory could give misleading results. For example, RdNBR from a relatively
441 open patch dominated by shorter canopy trees or shrubs and possessing relatively few giant
442 sequoias might indicate a high severity burn even if the fire did not do substantial damage to
443 taller giant sequoias. Additionally, RdNBR-derived estimates of giant sequoia regeneration
444 densities are highly variable at lower values (<640), leading to greater uncertainty in densities in
445 low to moderate severity burn patches – although, arguably, these areas are of less concern to
446 resource managers since canopy tree mortality is lower. Finally, other factors particular to a
447 given fire and time period might affect the relationship between RdNBR and seedling densities
448 (see ‘Large-scale and anomalous drivers of regeneration’). For these reasons, we strongly
449 suggest pairing RdNBR-based regeneration estimates with field validation to provide more
450 reliable estimates of post-fire giant sequoia regeneration densities for a given fire and year. For
451 example, how might these relationships change in relatively large groves that burned primarily at
452 high severity? How do differences in local factors (see ‘Uncaptured Mechanisms’) scale for
453 groves with different topographic profiles?

454

455 *Uncaptured Mechanisms*

456 There are mechanisms beyond local crown scorch that can affect interannual seedling
457 abundances within and between giant sequoia groves. In addition to among tree variation in seed
458 release, variability in abiotic factors such as topography (Marsh et al., 2022), soil characteristics

459 (Gates, 1982, Certini, 2005), fuels-mediated microsites (Gray & Spies, 1997), local climates
460 (e.g., aspect-driven) (Helgerson, 1990, Wolf et al., 2020) and moisture conditions (Stielstra et al.,
461 2015) can either facilitate or impede germination success – especially during the summer
462 immediately following wildfire when seedlings are most vulnerable to abiotic stressors
463 (Hartesveldt & Harvey, 1967, Harvey et al., 1980).

464 Anecdotal observations by our field crews indicated that high density patches of
465 seedlings within a plot often occurred within watercourse bottlenecks which function as moist
466 deposition sites for seeds caught in water runoff. In addition, high density patches were common
467 within soil compressions where a log was partially or fully combusted (see Harvey et al., 1980),
468 suggesting that pre-fire fuels can mediate post-fire seedling densities. Such mechanisms likely
469 help explain the substantial variability in seedling occurrence, even in areas which otherwise
470 appeared to have enough crown scorch to result in higher levels of seed release, and subsequent
471 high seedling densities. Importantly, these highly local effects might also have bearing on the
472 eventual success of maturing seedlings. For example, there is reason to question the viability of
473 even high-density patches of seedlings that occur near creek bottoms, as such areas are likely to
474 experience substantially increased stream flow, and subsequent mortality of initially established
475 seedlings, in high precipitation years.

476 Our data also indicate that – on rare occasions – patches of high seedling densities can
477 occur even when local crown conditions indicate otherwise. For example, one of the sampling
478 plots in the Board Camp grove had a particularly high seedling density, having more than double
479 (~2.2x) the count of any other plot, despite local crown scorch and RdNBR values indicating that
480 the availability of seeds should have been limited. Plausible explanations include the transport of
481 seeds from an area with higher seed production via seasonal stream flow and upslope seed rain

482 dispersal. The Board Camp grove is on a particularly steep slope (mean slope within grove:
483 27.7°) and is riddled with numerous drainages. Our ‘outlier’ plot was located within one of these
484 drainages (mean slope within plot: 34.4°) and downslope of trees with enough remaining
485 scorched crown volume to have potentially produced large numbers of viable seeds.

486

487 *Large-scale and anomalous drivers of regeneration*

488 Our results suggest that the burn severity metric RdNBR can be predictive of giant
489 sequoia seedling densities following wildfire. However, in addition to small-scale drivers
490 facilitating regeneration success, the magnitude of the relationship between burn severity and
491 seedling densities can be additively – and perhaps substantially– influenced by variation in more
492 global conditions such as trends in regional climate (see Avery et al., 2023) and their potential
493 interactions with giant sequoia ecology (Harvey et al., 1980). A recent climate assessment
494 encompassing all giant sequoia groves within Sequoia and Kings Canyon national parks
495 (Stephenson et al., in prep) found that the meteorological summers (June, July, August)
496 following the SQF and KNP wildfires were anomalously hot and dry, suggesting that seedlings
497 that germinated in 2021 and 2022 – in the summers following the 2020 SQF and 2021 KNP
498 wildfires – were subject to the 1st and 3rd hottest (mean °C), and 1st and 2nd driest (Palmer
499 Drought Severity Index, PDSI; Palmer, 1965) summers within the 121-year record.

500 Moreover, seed trap data from giant sequoia groves within Sequoia National Park
501 (Wright et al., 2021), along with NPS communications, suggest there was a region-wide seed
502 release event (non-masting) before the KNP wildfire, with ~10x increase in giant sequoia seed
503 fall relative to the annual mean of the prior 22 years (Stephenson et al., in prep). While giant
504 sequoias release viable seed year-to-year (Harvey et al. 1980, van Mantgem et al., 2006, Wright

505 et al., 2021), possibly triggered by the ambient feeding of Cerambycid beetles (*Phymatomes*
506 *nitidus*) and/or squirrels (e.g., *Tamiasciurus douglasii*) (Harvey et al., 1980), such an uptick in
507 seed release in the absence of fire-related stimuli is unprecedented. While causal mechanisms of
508 the seed release event are unknown, the extreme heat and aridity of the 2020 and 2021
509 meteorological summers may have induced a physiological response to release seed en masse.
510 Moreover, the mid-summer seed release in the absence of fire-mediated bare mineral soil would
511 not favor germination (Hartesveldt & Harvey, 1967, Stohlgren, 1993) and may have caused the
512 depletion of a significant portion of the seed stock before the ensuing KNP wildfire.

513 Given the extremely hot and dry climate window, when post-fire seed stock may have
514 been low, postfire seedling densities in the groves sampled here could be relatively low
515 compared to what might be found in cooler and wetter conditions and absent a prior large-scale
516 and likely unproductive seed release. As such, as noted above, it is important that any remote
517 sensing analysis is paired with robust ground data collection to provide an accurate
518 quantification of giant sequoia postfire regeneration after a given fire.

519 That said, we would expect RdNBR to remain a useful planning tool, regardless of other
520 factors. RdNBR should still be indicative of increasing giant sequoia mortality. In addition, the
521 metric should still have a relationship with tree scorch and torch, and therefore, local seed
522 availability. In other words, for any fire, we expect increasing RdNBR, at least within the range
523 of high severity, will be associated with increasing risk of grove area loss, with only the degree
524 of that risk varying with other conditions.

525

526 *Assessing long-term resilience*

527 While assessing seedling densities and the drivers of post-fire regeneration is important
528 for understanding the immediate trajectory of potential grove recovery, natural resource
529 managers are also understandably concerned with long-term grove resilience (DeRose & Long,
530 2014). Arguably, one of the best indicators of such resilience is the retention of seed-producing
531 trees—which allow for ‘second chances’ when a given regeneration cohort fails.

532 For example, high burn severities can facilitate conditions favorable for seed release and
533 soil conditions for germination – while simultaneously killing a large proportion of the seed
534 producing parent trees, resulting in a lack of resilience to future disturbance. Figure 4 shows that
535 high levels of postfire seedling germination can occasionally occur within high burn severity
536 areas (~800 RdNBR), while Figure 5 indicates that, at around the same RdNBR, the volume of
537 remaining live foliage and the probability of remaining live sequoias drops precipitously to near
538 zero. Given the decades of maturation required for sequoias to produce seed (Harvey et al., 1980;
539 see Sillett et al., 2019, Clark et al., 2021), large grove areas with high levels of seedling
540 germination but low levels of remaining live seed trees may not be resilient to near-term natural
541 disturbances (e.g., fire, drought, high precipitation). Even in typical conditions, natural
542 regeneration is subject to very high mortality, especially compared to nursery-grown seedlings,
543 which tend to survive at much higher rates, in part because they are planted at a maturation stage
544 which is less vulnerable to mortality from desiccation or erosion (York et al., 2007, Ouzts et al.,
545 2015, Marsh et al., 2021).

546 The location and size of fire-caused gaps in the context of the broader grove is also an
547 important consideration. Giant sequoia seedling germination and survivorship have been
548 associated with canopy gaps (Harvey et al., 1980, Stephenson et al., 1991, Demetry, 1995, Meyer
549 & Stafford, 2011, York et al., 2011); however, it is uncertain whether this association holds for

550 the large canopy gaps produced by the large high severity burn areas of recent fires (e.g., Cova et
551 al., 2022). Fire-produced gaps can facilitate germination and survivorship (Hartseveldt et al.,
552 1975, Harvey & Shellhammer, 1991, Shellhammer & Shellhammer, 2006) through increased
553 understory light penetration, exposed mineral soil, and removal of shade-tolerant competitors
554 from the forest understory (Harvey et al., 1980, Stephenson, 1994). However, larger gaps (e.g.,
555 more than a few hectares) contain areas considerably distant from the bulk of the seed shadow of
556 living sequoias (Clark et al., 2021), with these larger areas potentially experiencing a more
557 severe set of environmental conditions (e.g., reduced snow retention, see Stevens, 2017, Smoot
558 & Gleason 2021) that may have a negative, rather than positive, effect on giant sequoia seedling
559 germination and establishment. Moreover, gaps created at the edge of a grove boundary have less
560 perimeter adjacent to sequoias relative to gaps created internal to the grove boundary and are less
561 likely to receive giant sequoia seed. In short, deciding whether or not to plant after a fire involves
562 a nuanced assessment of seed tree mortality, post fire regeneration, probability of long-term
563 seedling survival, topography, and their spatial characteristics.

564

565 *Informing Management*

566 Giant sequoias present an interesting case study of how management challenges can
567 evolve through time and how science informs decision making. Decades ago, robust research on
568 giant sequoias led to the realization that over a century of fire suppression had resulted in
569 regeneration failure across much of the species' natural range (Kilgore and Biswell, 1971,
570 Harvey et al., 1980, Stephenson, 1994). This led managers to implement prescribed burning
571 programs to try to restore historical conditions and encourage more giant sequoia recruitment
572 (Stephenson, 1996). Ultimately, many groves were not reached by these programs. Now, groves

573 that haven't burned in well over a century are experiencing fires of a severity well outside the
574 historical norm, and our research suggests that such fires have a substantial probability of
575 resulting in loss of grove area. In other words, managers may now be asking whether giant
576 sequoia conservation might best involve, not only prescribed burning, but also planting. As such
577 novel conditions occur, managers often have an increased need for real time data and
578 comparisons with past conditions to inform management decisions.

579 In deciding whether to intervene, managers may balance agency management goals,
580 directives, and budgets against the risk of permanent giant sequoia grove loss, and they may have
581 only limited time to do so, as growth of shrubs in high severity burn patches could rapidly make
582 proposed replanting areas inaccessible. For an agency like the National Park Service, especially
583 managing within designated wilderness areas, this may include balancing goals and directives to
584 maintain giant sequoia groves unimpaired for future generations with a desire to minimize
585 human intervention. This decision-making is complicated by the fact that there is not enough
586 information to set a precise minimum threshold that will guarantee regeneration success, and,
587 even if there were, the inherent uncertainty in sampling seedling densities will always leave
588 uncertainty in whether any given threshold has actually been met.

589 Traditional statistical approaches, which test mean estimates against a particular
590 threshold at an arbitrary level of confidence, are not ideally suited to such situations. First, in a
591 circumstance without definitive thresholds, managers are best served by approaches that allow
592 simultaneous consideration of a variety of potential thresholds that can be determined based on
593 the management context (e.g., the level of seed tree mortality or the degree of public resistance
594 to intervention). Furthermore, in a conservation context, managers are more likely to ask, 'What

595 is the probability that there are plenty of seedlings?’ rather than ‘Can I prove with 95%
596 confidence that my seedling densities are not high enough?’

597 In this study, we used a Bayesian statistical framework that allows us to assess
598 probabilities of meeting any given management-relevant threshold (see Stephenson et al., in
599 prep) while also explicitly quantifying the uncertainty (which is affected both by data variability
600 and richness). Moreover, Bayesian modeling offers a more flexible and interpretable tool for
601 managers to use in the context of conservation, where decision making can be inherently
602 subjective and challenging. Such an approach allows managers to explore a range of risk
603 tolerances. For example, do we only want to intervene if there is less than a 25% probability that
604 regeneration that the mean seedling density falls above the threshold for successful regeneration,
605 or would we choose a higher threshold because we consider the consequences of regeneration
606 failure and the lost opportunity to act within the natural regeneration window of giant sequoia
607 too great? Decisions regarding what risk level to set can involve tradeoffs between costs of
608 action versus costs of inaction made in the context of agency mandates, law, policy, and budgets.
609 Having clearly identified probabilities regarding whether the mean is likely to meet an identified
610 target can be very helpful in these contexts. Managers may find this level of explicit risk analysis
611 helpful in tackling these difficult conservation and management decisions.

612

613 *Conclusion*

614 Increasingly, forests in the Sierra Nevada are experiencing wildfires well outside the
615 historical norm, with such fires affecting vast landscapes and potentially leading, without
616 intervention, to permanent changes in vegetation composition and structure (Safford and Stevens
617 2017). Managers are faced with responding to these events and deciding whether to intervene —

618 often with only short windows in which action can be implemented practically and in the face of
619 enormous uncertainty and public concern. Such circumstances demand robust data collection
620 efforts combined with analyses designed to quantify uncertainty in a way that is usable and
621 informative for managers who must make pragmatic assessments about whether to act.

622 Here, we assessed post-fire regeneration within four different giant sequoia groves
623 significantly affected by the SQF- (2020) and KNP-Complex (2021) fires. We found significant
624 spatial relationships between giant sequoia seedling densities, neighborhood crown conditions,
625 and the remotely-sensed burn severity metric, RdNBR – and used those relationships to scale
626 predictions of giant sequoia mortality and regeneration across unsampled grove areas along a
627 gradient of high burn severity. To help inform natural resource managers, we developed a
628 Bayesian probabilistic modeling approach that directly quantifies the uncertainty surrounding
629 modeled estimates of post-fire regeneration that could potentially be scaled across groves and
630 different fires.

631 Overall, this study advances our understanding of giant sequoia ecology, and provides a
632 statistical tool for informing management decisions regarding postfire restoration following
633 severe, large wildfires. Going forward, if we to are gain a deeper understanding of giant sequoia
634 regeneration in this new era, we will need to tease apart the relationships that drive high
635 heterogeneity of seed germination on the landscape and gain a far better handle on the likely
636 survivorship of such seedlings in the long-term.

637

638 ACKNOWLEDGEMENTS

639 We thank the many people involved in collecting field data, specifically the U.S.
640 Geological Survey, Sequoia & Kings Canyon National Parks, and University of California,
641 Davis field crews, and those maintaining the critical information used in this study. We also
642 thank the Sequoia & Kings Canyon National Parks and the University of California, Merced
643 SCICON (Science & Conservation) Field Stations for logistical support, and Martin Holdrege for
644 statistical help. We are continually appreciative of the Sequoia National Park staff for decades of
645 invaluable cooperation. This research was funded by the NPS, and the U.S. Geological Survey
646 Ecosystems and Climate and Land Use Research and Development programs. Any use of trade,
647 firm, or product names is for descriptive purposes only and does not imply endorsement by the
648 U.S. Government.

649

650
651
652
653
654
655
656
657
658
659
660
661
662
663
664
665
666
667
668
669
670
671
672
673
674
675
676
677
678
679

LITERATURE CITED

Avery, P.H., C.J. Nolan, K.S. Hemes, T.W. Cambron, and C.B. Field. 2023. Low-elevation conifers in California’s Sierra Nevada are out of equilibrium with climate. *PNAS Nexus* 2: pgad004.

Certini, G. 2005. Effects of fire on properties of forest soils: A review. *Oecologia* 143, 1–10.

Clark, J.S., R. Andrus, M. Aubry-Kientz, Y. Bergeron, M. Bogdziewicz, D.C. Bragg, D. Brockway, N.L. Cleavitt, S. Cohen, B. Courbaud, R. Daley, A.J. Das, M. Dietze, T.J. Fahey, I. Fer. J.F. Franklin, C.A. Gehring, G.S. Gilbert, C.H. Greenberg, Q. Guo, J. HilleRisLambers, I. Ibanez, J. Johnstone, C.L. Kilner, J. Knops, W.D. Koenig, G. Kunstler, JLaMontagne, K.L. Legg, J. Luongo, J.A. Lutz, D. Macias, E.J.B. McIntire, Y. Messaoud, C.M. Moore, E. Moran, J.A. Myers, O.B. Myers, C. Nunez, R. Parmenter, S. Pearse, S. Pearson, R. Poulton-Kamakura, E. Ready, M.D. Redmond, C.D. Reid, K.C. Rodman, C.L. Scher, W.H. Schlesinger, A.M. Schwantes, E. Shanahan, S. Sharma, M.A. Steele, N.L. Stephenson, S. Sutton, J.J. Swenson, m. Swift, T.T. Veblen, A.V. Whipple, T.G. Whitham, A.P. Wion, K. Zhu, and R. Zlotin. 2021. Continent-wide tree fecundity driven by indirect climate effects. *Nature Communications* 12: 1242.

Cova, G. Kane, V.R., Prichard, S., North, M., and A.C. Cansler. 2023. The outsized role of California’s largest wildfires in changing forest burn patterns and coarsening ecosystem scale. *Forest Ecology and Management* 528: 120620.

Demetry, A. 1995. Regeneration patterns within canopy gaps in a giant sequoia mixed conifer forest: implications for forest restoration. Masters thesis, Northern Arizona University.

DeRose, R.J., and J.N. Long. 2014. Resistance and Resilience: A Conceptual Framework for Silviculture. *Forest Science* 60: 1205–1212.

Fassnacht, F.E., E. Schmidt-Riese, T. Kattenborn, and J. Hernández. 2021. Explaining Sentinel 2-based dNBR and RdNBR variability with reference data from the bird’s eye (UAS) perspective. *International Journal of Applied Earth Observation and Geoinformation* 95: 102262.

Gates, D.M. 1982. Biophysical Ecology. Courier Corporation.

Gelman, A. and D.B. Rubin. 1992. Inference from Iterative Simulation Using Multiple Sequences. *Statistical Science* 7: 457–472.

680 Goodrich B, Gabry J, Ali I, Brilleman S. 2022. rstanarm: Bayesian applied regression modeling
681 via Stan. R package version 2.21.3.

682 Gray, A.N. and T.A Spies. 1997. Microsite controls on tree seedling establishment in conifer
683 forest canopy gaps. *Ecology* 78: 2458–2473.

684 Haggmann, R.K., P.F. Hessburg, S.J. Prichard, N.A. Povak, P.M. Brown, P.Z. Fulé, R.E. Keane,
685 E.E. Knapp, J.M. Lydersen, K.L. Metlen, M.J. Reilly, A.J. Sánchez Meador, S.L. Stephens,
686 J.T. Stevens, A.H. Taylor, L.L. Yocom, M.A. Battaglia, D.J. Churchill, L.D. Daniels, D.A.
687 Falk, P. Henson, J.D. Johnston, M.A. Krawchuk, C.R. Levine, G.W. Meigs, A.G. Merschel,
688 M.P. North, H.D. Safford, T.W. Swetnam, and A.E.M. Waltz. 2021. Evidence for widespread
689 changes in the structure, composition, and fire regimes of western North American forests.
690 *Ecological Applications* 31, e02431.

691 Hart, R. 2023. Giant Sequoia Groves of the Sierra Nevada California.
692 <https://www.fs.usda.gov/wps/portal/fsinternet3/cs/detail/r5/landmanagement/gis/>

693 Hartesveldt, R.J. and H.T. Harvey. 1967. The fire ecology of Sequoia regeneration. Pp. 65-77 in Tall
694 Timbers Fire Ecology Conference No. 7. Tall Timbers Research Station. Tallahassee, FL.

695 Hartesveldt, R.J., H.T. Harvey, H.S. Shellhammer, and R.E. Stecker. 1975. The giant sequoia of
696 the Sierra Nevada. Department of the Interior, National Park Service, Washington, D.C.,
697 USA.

698 Harvey, H.T., H.S. Shellhammer, and R.E. Stecker. 1980. Giant sequoia ecology. US
699 Department of the Interior National Park Service, Washington, D.C., USA.

700 Harvey, H.T. and H.S. Shellhammer. 1991. Survivorship and growth of Giant Sequoia (*Se-*
701 *quoiadendron giganteum* (Lindl.) Buchh.) seedlings after fire. *Madroño* 38:14–20.

702 Helgerson, O. T. 1990. Heat damage in tree seedlings and its prevention. *New Forests* 3: 333–
703 358.

704 Hoy, E.E., N.H. French, M.R. Turetsky, S.N. Trigg, and E.S. Kasaschke. 2008. Evaluating the
705 potential of Landsat TM/EIM+ imagery for assessing fire severity in Alaskan black spruce
706 forest. *International Journal of Wildland Fire* 17: 500–514.

707 Keeley, J.E., Syphard, A.D., 2021. Large California wildfires: 2020 fires in historical context.
708 *Fire Ecology* 17, 22.

709 Kilgore, B.M., and H.H. Biswell. 1971. Seedling germination following fire in a giant sequoia
710 forest. *California Agriculture* 25: 8–10.

711 Marsh, C., J.L. Crockett, D. Krofcheck, A. Keyser, C.D. Allen, M. Litvak, and M.D. Hurteau.
712 2022. Planted seedling survival in a post-wildfire landscape: From experimental planting to
713 predictive probabilistic surfaces. *Forest Ecology and Management* 525, 120524.

714 Meyer, M. and H. Safford. 2011. Giant sequoia regeneration in groves exposed to wildfire and
715 retention harvest. *Fire Ecology* 7: 2–16.

716 Miller, J.D. and A.E. Thode. 2007. Quantifying burn severity in a heterogeneous landscape with
717 a relative version of the delta Normalized Burn Ratio (dNBR). *Remote Sensing of the*
718 *Environment* 109: 66–80.

719 Miller JD, Quayle B. 2015. Calibration and validation of immediate post-fire satellite-derived
720 data to three severity metrics. *Fire Ecology* 11: 12–30.

721 MTBS Data Access: Fire Level Geospatial Data. (2017, July - last revised). MTBS Project
722 (USDA Forest Service/U.S. Geological Survey).

723 Ouzts, J., T. Kolb, D. Huffman, and A.S. Meador. 2021. Post-fire ponderosa pine regeneration
724 with and without planting in Arizona and New Mexico. *Forest Ecology and Management*
725 354: 281–290.

726 Palmer, W.C. 1965. Meteorological drought Research Paper No. 45, US Department of
727 Commerce Weather Bureau, Washington, D.C., USA, 58 pp.

728 Parks, S.A. and J.T. Abatzoglou. 2020. Warmer and drier fire seasons contribute to increases in
729 area burned at high severity in western US forests from 1985 to 2017. *Geophysical Research*
730 *Letters* 47, e2020GL089858.

731 R Core Team. 2022. R: A language and environment for statistical computing. R
732 Foundation for Statistical Computing, Vienna, Austria. URL
733 <https://www.R-project.org/>.

734 Rapid Assessment of Vegetation Condition after Wildfire (RAVG) Composite Burn Index (Map
735 Service). U.S. Forest Service.

736 Safford, H.D and J.T. Stevens. 2017. Natural range of variation for yellow pine and mixed-
737 conifer forests in the Sierra Nevada, southern Cascades, and Modoc and Inyo National
738 Forests, California, USA. Gen. Tech. Rep. PSW-GTR-256. Albany, CA: U.S. Department of
739 Agriculture, Forest Service, Pacific Southwest Research Station. 229 p.

740 Safford, H.D., Paulson, A.K., Steel, Z.L., Young, D.J.N., Wayman, R.B., Varner, M. 2022. The
741 2020 California fire season: A year like no other, a return to the past or a harbinger of the
742 future? *Global Ecology and Biogeography* 31: 2005–2025.

743 Sequoia Tree Inventory Sequoia and Kings Canyon national parks California, prepared for US
744 DOI, NPS, Sequoia and Kings Canyon national parks, Three Rivers, California, by Hammon,
745 Jensen & Wallen Mapping and Forestry Services, Oakland CA, 1964 & 1973, and Western
746 Timber Service, Arcata CA, 1967, scale of 1:2400.

747 Shellhammer, H.S. and T.H. Shellhammer. 2006. Giant sequoia (*Sequoiadendron giganteum*
748 [Taxodiaceae]) seedling survival and growth in the first four decades following managed
749 fires. *Madroño* 53: 342–350.

750 Shive, K.L., H.K. Preisler, K.R. Welch, H.D. Safford, R.J. Butz, K.L. O’Hara, and S.L.
751 Stephens. 2018. From the stand scale to the landscape scale: predicting the spatial patterns of
752 forest regeneration after disturbance. *Ecological Applications* 28: 1626–1639.

753 Shive, K.L., A. Wuenschel, L.J. Hardlund, S. Morris, M.D. Meyer, S.M. Hood. 2022. Ancient
754 trees and modern wildfires: Declining resilience to wildfire in the highly fire-adapted giant
755 sequoia. *Forest Ecology and Management* 511, 120110.

756 Sillett., S.C., R. Van Pelt, A.L. Carroll, R.D. Kramer, A.R. Ambrose, and D. Trask. 2015. How
757 do tree structure and old age affect growth potential of California redwoods? *Ecological*
758 *Monographs* 85: 181–212.

759 Sillett, S.C., Van Pelt, R., Carroll, A.L., Campbell-Spickler, J., and Antoine, M.E. 2019.
760 Structure and dynamics of forests dominated by *Sequoiadendron giganteum*, *Forest Ecology*
761 *and Management* 448: 218–239.

762 Smoot, E.E., and K.E. Gleason. 2021. Forest fires reduce snow-water storage and advance the
763 timing of snowmelt across the Western U.S. *Water* 13: 3533.

764 Stan Development Team. 2023. “RStan: the R interface to Stan.” R package version 2.21.8,
765 <https://mc-stan.org/>.

766 Stark, N. 1968. Seed Ecology of *Sequoiadendron giganteum*. *Madroño* 19: 267–277.

767 Steel, Z.L., Jones, G.M., Collins, B.M., Green, R., Koltunov, A., Purcell, K.L., Sawyer, S.C.,
768 Slaton, M.R., Stephens, S.L., Stine, P., and C. Thompson. 2022. Mega-disturbances cause
769 rapid decline of mature conifer forest habitat in California. *Ecological Applications* E2763.

770 Stephens, S.L., Martin, R.E., and N.E. Clinton. 2007. Prehistoric fire area and emissions from
771 California's forests, woodlands, shrublands, and grasslands. *Forest Ecology and*
772 *Management* 251: 205–216.

773 Stephens, S.L., Bernal, A.A., Collins, B.M., Finney, M.A., Lautenberger, C., and D. Saah. 2022.
774 Mass fire behavior created by extensive tree mortality and high tree density not predicted by
775 operational fire behavior models in the southern Sierra Nevada. *Forest Ecology and*
776 *Management* 518, 120258.

777 Stephenson, N.L., D.J. Parsons, and T.W. Swetnam. 1991. Restoring natural fire to the sequoia-
778 mixed conifer forest: should intense fire play a role? Proceedings of the 17th Tall Timbers
779 Fire Ecology Conference 17: 321–337.

780 Stephenson, N.L. 1994. Long-term dynamics of giant sequoia populations: implications for
781 managing a pioneer species. Pages 56–63 in: P.S. Aune, technical coordinator. The
782 symposium on giant sequoias: their place in the ecosystem and society. USDA Forest Service
783 Pacific Southwest Research Station General Technical Report PSW-GTR-151, Albany,
784 California, USA.

785 Stephenson, N.L. 1996. Ecology and Management of Giant Sequoia Groves. Chapter 55 in SNEP
786 Report.

787 Stephenson, N.L. 2000. Estimates ages of some large giant sequoias: General Sherman keeps
788 getting younger. *Madroño* 47: 61–67.

789 Stevens, D.L. and A.R. Olsen. 2004. Spatially Balanced Sampling of Natural Resources, *Journal*
790 *of the American Statistical Association* 99: 262–278.

791 Stevens, J.T. 2017. Scale-dependent effects of post-fire canopy cover on snowpack depth in
792 montane coniferous forests. *Ecological Applications* 27: 1888–1900.

793 Stevens, J.T., B.M. Collins, J.D. Miller, M.P. North, and S.L. Stephens. 2017. Changing spatial
794 patterns of stand replacing fire in California conifer forests. *Forest Ecology and Management*
795 406: 28–36.

796 Stielstra, C.M., K.A. Lohse, J. Chorover, J.C. McIntosh, G.A. Barron-Gafford, J.N. Perdrial, M.
797 Litvak, H.R. Barnard, and P.D. Brooks. 2015. Climatic and landscape influences on soil
798 moisture are primary determinants of soil carbon fluxes in seasonally snow-covered forest
799 ecosystems. *Biogeochemistry* 123: 447–465.

800 Stohlgren, T.J. 1993. Spatial patterns of giant sequoia (*Sequoiadendron giganteum*) in two
801 sequoia groves in Sequoia National Park, California. *Canadian Journal of Forest Research*
802 23: 120–132

803 Swetnam, T.W., C.H. Baisan, A.C. Caprio, P.M. Brown, R. Touchan, R.S. Anderson, and D.J.
804 Hallett. 2009. Multi-millennial fire history of the Giant Forest, Sequoia National Park,
805 California, USA. *Fire Ecology* 5: 120–150.

806 Verbyla, D.L., E.S. Kasischke, and E.E. Hay. 2008. Seasonal and topographic effects on
807 estimating fire severity from landsat TM/EMT+ data. *International Journal of Wildland Fire*
808 17: 527–534.

809 Westerling, A.L. 2016. Increasing western US forest wildfire activity: Sensitivity to changes in
810 the timing of spring. *Philosophical Transactions of the Royal Society B: Biological Sciences*
811 371, 20150178.

812 Wright, M.C., P. van Mantgem, N.L. Stephenson, A.J. Das, and J.E. Keeley. 2021. Seed
813 production patterns of surviving Sierra Nevada conifers show minimal change following
814 drought. *Forest Ecology and Management* 480, 118598.

815 Wolf, K.D., P.E. Higuera, K.T. Davis, and S.Z. Dobrowski. 2021. Wildfire impacts on forest
816 microclimate vary with biophysical context. *Ecosphere* 12, e03467.

817 York RA, Battles JJ, Heald RC. 2007. Gap-based silviculture in a sierran mixed-conifer forest:
818 effects of gap size on early survival and 7-year seedling growth. In: Powers, Robert F., tech.
819 editor. Restoring fire-adapted ecosystems: proceedings of the 2005 national silviculture
820 workshop. General Technical Report PSW-GTR-203, Albany, CA: Pacific Southwest
821 Research Station, Forest Service, U.S. Department of Agriculture: p. 181–191.

822 York, R.A., J.J. Battles, A.K. Eschtruth, and R.G. Schurr. 2011. Giant Sequoia (*Sequoiadendron*
823 *giganteum*) Regeneration in Experimental Canopy Gaps. *Restoration Ecology* 19: 14–23.

824 York, R.A., N.L. Stephenson, M.D. Meyer, S. Hanna, M. Tadashi, A.C. Caprio, and J.J. Battles.
825 2013. A natural resource condition assessment for Sequoia and Kings Canyon national parks:
826 Appendix 11a: giant sequoias.

827

FIGURES

828
829
830
831
832
833
834
835

Figure 1. A) Fire-killed giant sequoias (*Sequoiadendron giganteum*) and other conifers in the Board Camp Grove, Sequoia National Park. B) Ground view of giant sequoia and other conifers in the Board Camp Grove, Sequoia National Park. Note the fire-killed ‘monarch’ giant sequoia (~500cm diameter at breast height) in the foreground. C) Cluster of fire-killed giant sequoias in Redwood Meadow Grove. Photo Credits: (A) Tony Caprio, NPS; (B,C) David Soderberg, USGS.

836 Figure 2. Study plot locations (red circles, triangles*) within Board Camp, Redwood Mountain,
837 Suwane, and New Oriole Lake giant sequoia (*Sequoiadendron giganteum*) groves within
838 Sequoia and Kings Canyon national parks, CA**. Locations were drawn using the Generalized
839 Random Tessellation Stratified (GRTS) algorithm (Stevens & Olsen, 2004) using an equal
840 probability stratified sampling design within the entirety of Board Camp, Suwane, and New
841 Oriole Lake groves, but confined to the ‘high’ burn severity (>75% basal area loss; see Rapid
842 Assessment of Vegetation Condition after Wildfire (RAVG);
843 <https://burnseverity.cr.usgs.gov/ravg/>) regions of Redwood Mountain grove. RdNBR-categorized
844 burn severity raster pixels are presented in greyscale (white = low severity, <25% basal area loss;
845 light and dark grey = moderate severity, 26-75% basal area loss; black = high severity or
846 unburned, >75% basal area loss).
847 * Plots in Board Camp, Suwane, and New Oriole Lake groves are scaled to represent the actual
848 area surveyed. Plots in Redwood Mountain grove (triangles) are, for visibility, scaled larger than
849 their actual sizes.
850 ** Redwood Mountain map includes US Forest Service and state land that was not part of our
851 sampling area.

852 Figure 3. Predicted mean regeneration (seedlings/hectare) for groves affected by the 2021 KNP-
853 Complex (i.e., Redwood Mountain, Suwane, and New Oriole Lake groves) and 2020 SQF-
854 Complex fires (i.e., Board Camp). For each sampled grove, the probabilities of the true mean
855 regeneration density (i.e., seedlings/ha) being larger than specified seedling counts are shown
856 (see Table 1). Bayesian 90% credible intervals are highlighted in grey.

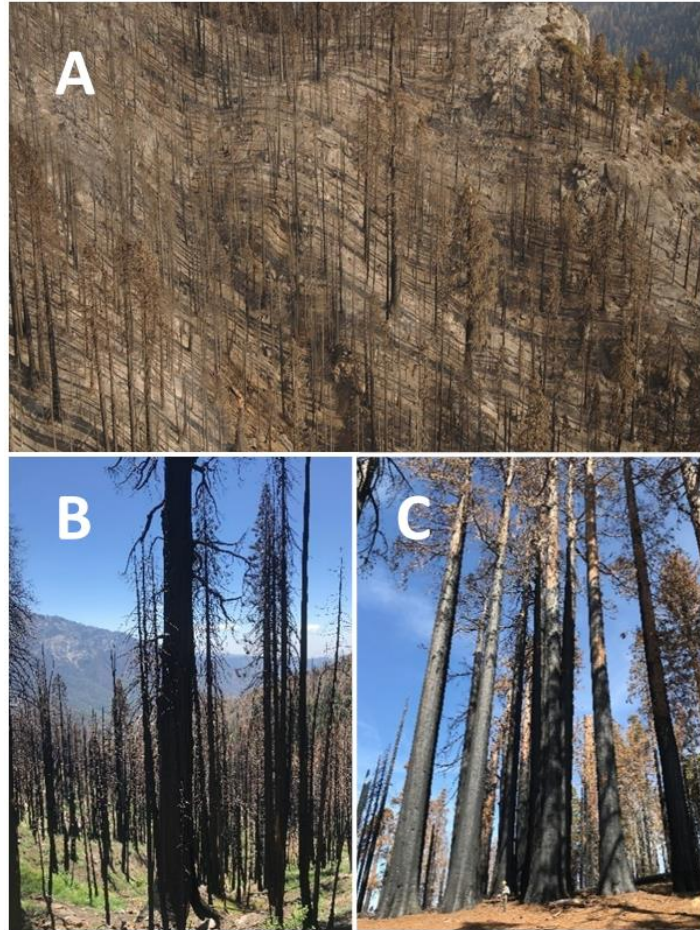
857 Figure 4. Top panels: predicted mean regeneration (seedlings/hectare) for groves affected by the
858 2021 KNP-Complex (i.e., Redwood Mountain, Suwane, and New Oriole Lake) and the 2020
859 SQF-Complex fires (i.e., Board Camp) as a function of RdNBR values (first row). Bottom
860 panels: predicted mean regeneration densities (seedlings/ha) at specified RdNBR values (see
861 Table 2).

862 Figure 5. Neighborhood crown volumes (within 50 meters of plot center) of giant sequoia live,
863 scorched, and torched foliage as a function of remote-sensed derived RdNBR values. Individual
864 tree crown volumes were calculated using allometric equations derived from Sillett et al., 2019
865 measurements (see Appendix S1: Equation S1) and calculated using observed crown proportion
866 of live, scorch, and torch and location data from this study.

867 Figure 6. Giant sequoia stem map and categorized RdNBR areas for surveyed groves – Board
868 Camp, Redwood Mountain, Suwane, and New Oriole Lake Groves, Sequoia and Kings Canyon

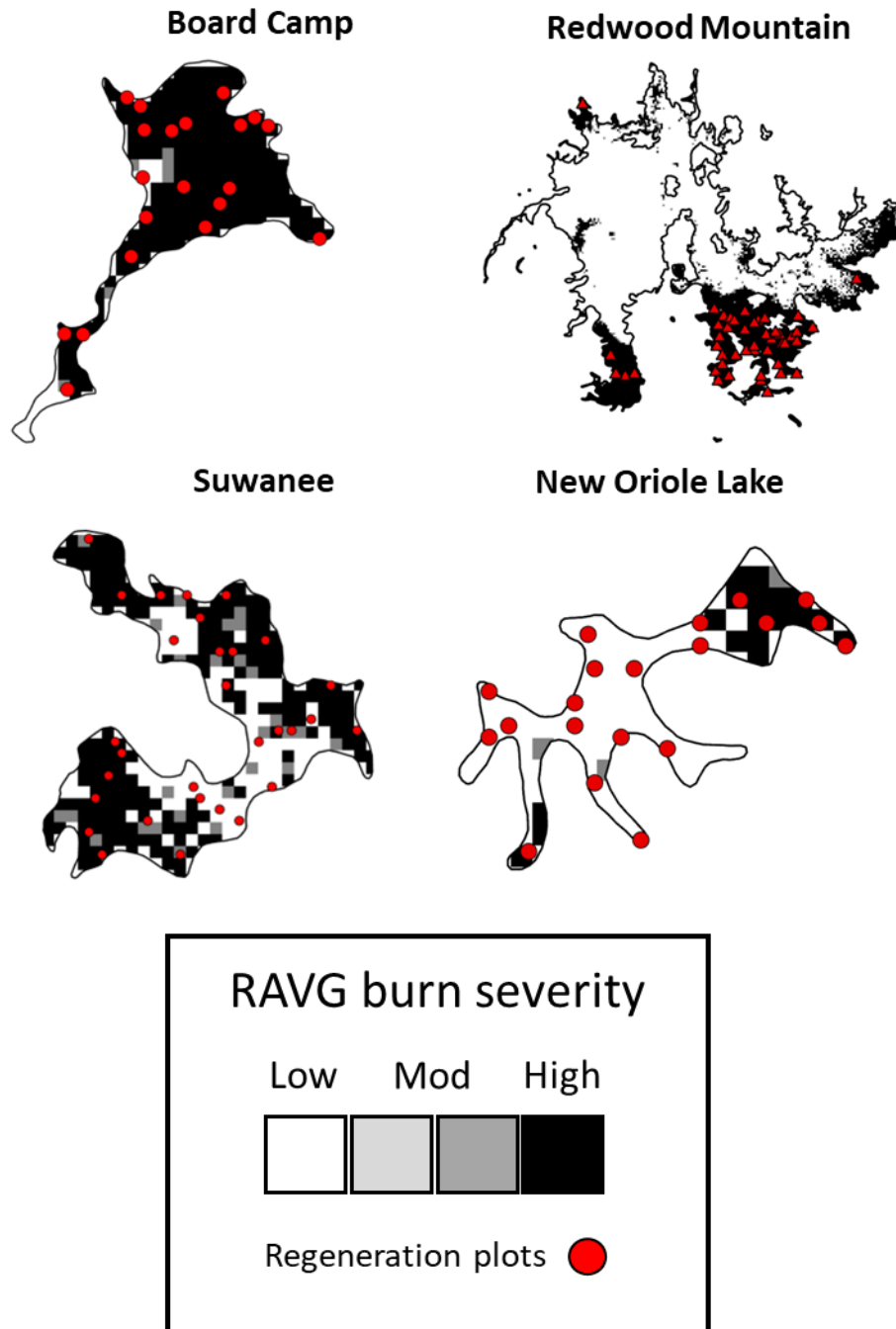
869 national parks, CA. Mapped giant sequoias are color coded by live/dead status: Black = live,
870 white = dead (individual giant sequoia within Redwood Mountain not visualized due to grove
871 size). Grove regions with RdNBR values > 800 are colored in red, with increasingly dark color
872 tone with increasing RdNBR values.

873

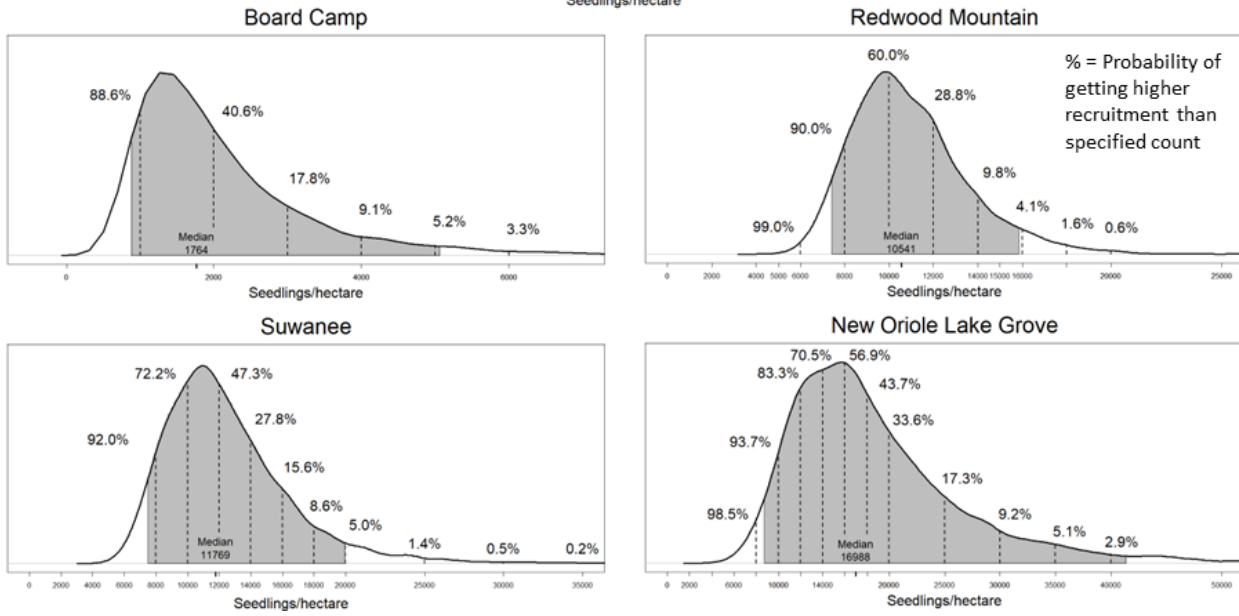
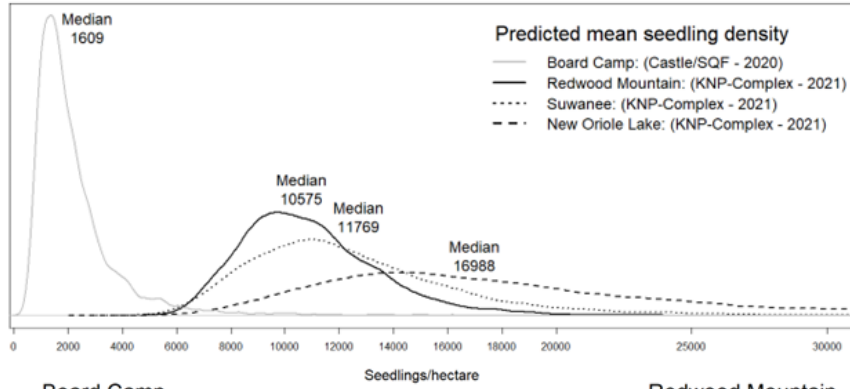


874

875 **Figure 1**

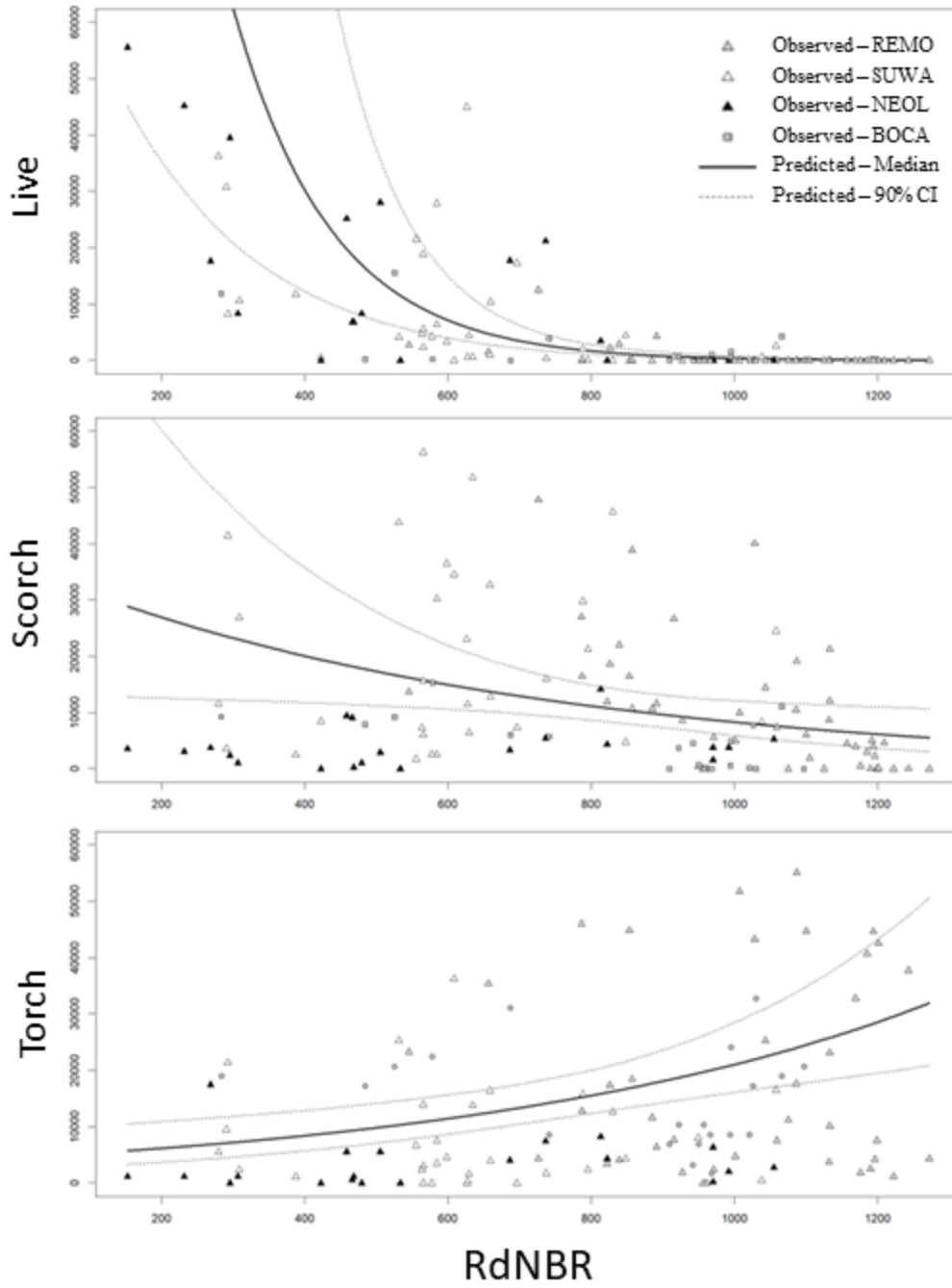


876
877 **Figure 2**



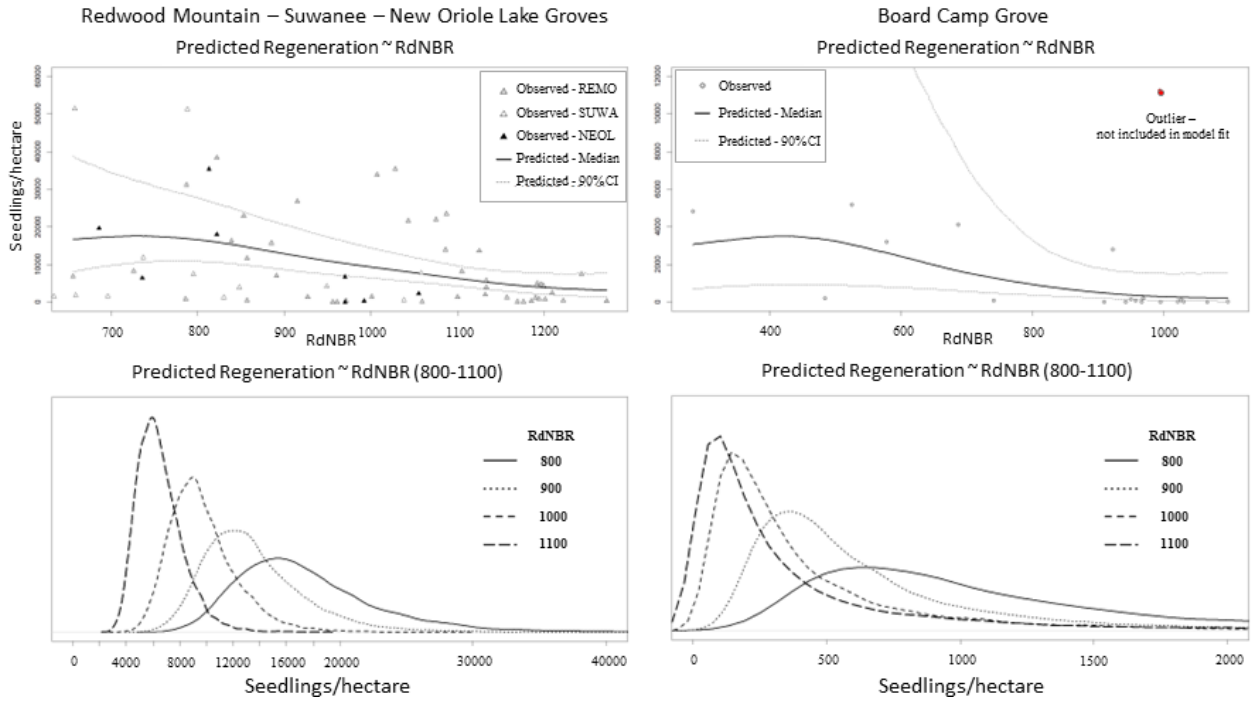
878
879 **Figure 3**

Neighborhood Crown Volume (m^3)



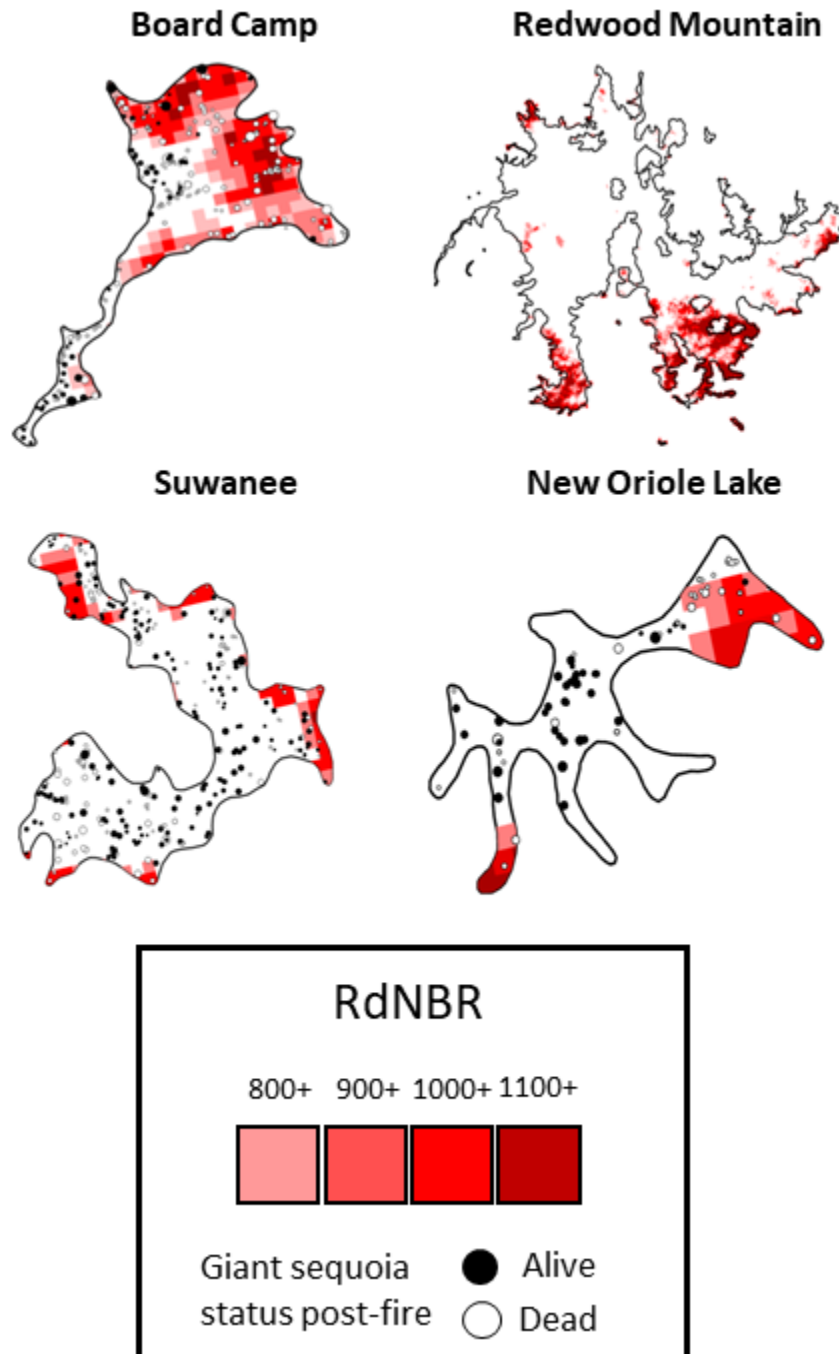
880

881 **Figure 4**



882

883 **Figure 5**



884

885 **Figure 6**

886

TABLES

887 Table 1. Mean regeneration densities and Bayesian probabilities of mean regeneration densities
 888 meeting (i.e, are greater than or equal to) the specified seedlings/hectare for each grove. See
 889 *Methods – Statistical Analysis* for details. Probabilities that are <10% are highlighted in grey.

Fire/year	Grove	Raw data	Bayesian probabilities (italics) of mean regeneration densities meeting specified seedlings/hectare (bold) for each grove									
			Seedlings/hectare									
SQF 2020	Board Camp	Mean	1000	2000	3000	4000	5000	6000	8000	10000	12000	
		1611	<i>87.7</i>	<i>41.6</i>	<i>18.5</i>	<i>9.8</i>	<i>5.7</i>	<i>3.4</i>	<i>1.5</i>	<i>0.8</i>	<i>0.5</i>	
KNP Complex 2021	Redwood Mountain*	10363	<i>90.0</i>	<i>60.0</i>	<i>28.8</i>	<i>9.8</i>	<i>4.1</i>	<i>1.6</i>	<i>0.5</i>	<i><0.1</i>	<i>0</i>	
	Suwanee	11435	<i>92.0</i>	<i>72.2</i>	<i>47.3</i>	<i>27.8</i>	<i>15.6</i>	<i>8.6</i>	<i>5.0</i>	<i>1.4</i>	<i>0.5</i>	
	New Oriole Lake	16080	<i>98.5</i>	<i>93.7</i>	<i>83.3</i>	<i>70.5</i>	<i>56.9</i>	<i>43.7</i>	<i>33.6</i>	<i>17.3</i>	<i>9.2</i>	

890 * Redwood Mountain plot locations were restricted to areas of high burn severity (RdNBR >640)

891

892 Table 2. Bayesian probability estimates of mean regeneration densities as a function of RdNBR
 893 (relativized differenced normalized burn ratio; Miller & Thode, 2007). See *Methods* for details.
 894 Probability estimates represent the probability of meeting (greater than or equal to) the specified
 895 seedlings/hectare for a given RdNBR value. Probabilities that are <10% are highlighted in grey.

		Bayesian probabilities (<i>italics</i>) of mean regeneration densities meeting specified seedlings/hectare (bold) as a function of RdNBR values							
Fire/year	Grove	RdNBR	Seedlings/hectare						
			1000	2000	3000	4000	5000	6000	
SQF 2020	Board Camp (w/o outlier*)	800	<i>45.8</i>	<i>14.9</i>	<i>6.8</i>	<i>3.7</i>	<i>2.1</i>	<i>1.5</i>	
		850	<i>29.0</i>	<i>7.5</i>	<i>2.9</i>	<i>1.6</i>	<i>0.9</i>	<i>0.5</i>	
		900	<i>17.4</i>	<i>4.2</i>	<i>1.7</i>	<i>0.8</i>	<i>0.5</i>	<i>0.2</i>	
		950	<i>12.2</i>	<i>3.1</i>	<i>1.3</i>	<i>0.7</i>	<i>0.4</i>	<i>0.2</i>	
		1000	<i>10.0</i>	<i>2.9</i>	<i>1.3</i>	<i>0.8</i>	<i>0.4</i>	<i>0.2</i>	
		1050	<i>10.5</i>	<i>2.9</i>	<i>1.4</i>	<i>0.7</i>	<i>0.5</i>	<i>0.3</i>	
		1100	<i>10.2</i>	<i>3.2</i>	<i>1.5</i>	<i>0.8</i>	<i>0.5</i>	<i>0.4</i>	
			8000	10000	12000	14000	16000	18000	
KNP Complex 2021	Redwood Mountain - Suwanee - New Oriole Lake (combined**)	800	<i>99.7</i>	<i>97.4</i>	<i>88.5</i>	<i>73.4</i>	<i>55.1</i>	<i>38.4</i>	
		850	<i>99.4</i>	<i>94.7</i>	<i>80.6</i>	<i>59.2</i>	<i>39.1</i>	<i>24.5</i>	
		900	<i>97.5</i>	<i>84.6</i>	<i>60.8</i>	<i>36.6</i>	<i>21.0</i>	<i>11.4</i>	
		950	<i>90.5</i>	<i>64.2</i>	<i>35.9</i>	<i>17.9</i>	<i>8.2</i>	<i>3.8</i>	
		1000	<i>74.5</i>	<i>38.2</i>	<i>16.3</i>	<i>6.0</i>	<i>2.3</i>	<i>0.9</i>	
		1050	<i>45.7</i>	<i>15.6</i>	<i>4.7</i>	<i>1.3</i>	<i>0.4</i>	<i>0.1</i>	
		1100	<i>17.0</i>	<i>3.6</i>	<i>0.8</i>	<i>0.2</i>	<i><0.1</i>	<i><0.1</i>	

896 * Model estimates calculated with outlier removed. See Figure 5 for all data visualization.

897 ** Model estimates calculated within areas of high severity (RdNBR >640).

898

APPENDIX S1

899
900
901
902
903
904
905
906
907
908
909
910
911
912
913
914
915
916
917
918
919

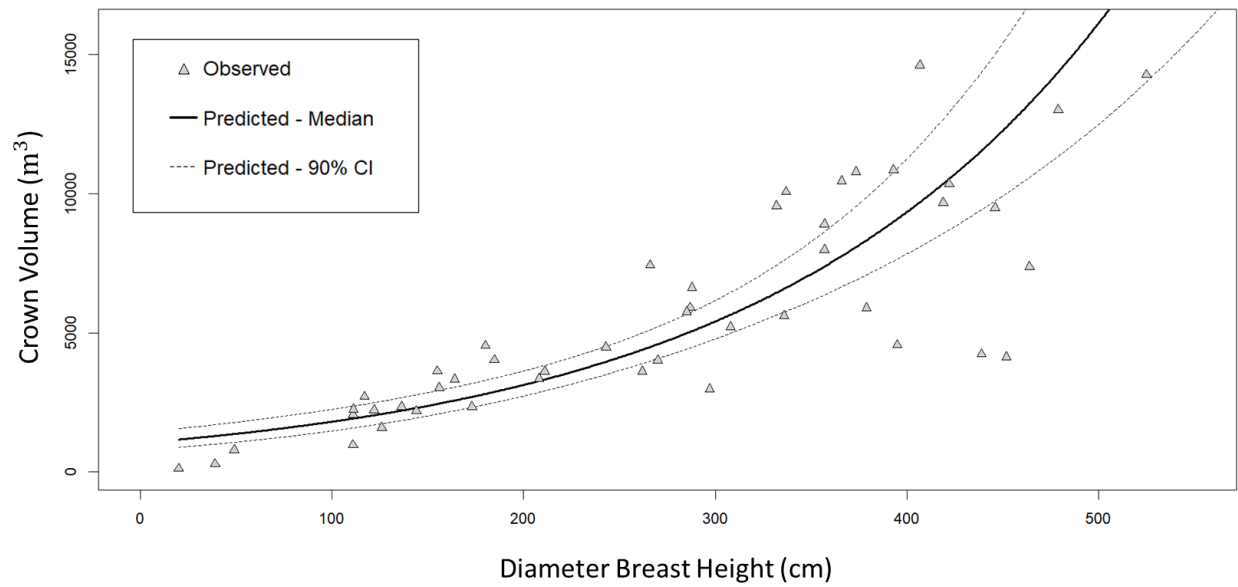
We used a negative binomial count model to calculate estimates of the relationship between diameter breast height (cm) and crown volume (m³) based on data published in Sillett et al., 2019 (Figure S1). The median estimate for the modeled relationship is described with the following:

$$\log(y) = 6.953 + 0.00547*(\text{diameter in centimeters}) \quad (\text{S1})$$

and was used as an allometric equation for estimating crown volumes for the giant sequoia assessed within our study.

In addition, we calculated estimates of the relationships between regeneration density (seedlings/hectare) and neighborhood crown volume scorch (first row) and neighborhood crown volume scorch and RdNBR (second row), separating analyses by groves that were affected by different fires/years (column 1: KNP-complex [2021] affected Redwood Mountain, Suwanee, and New Oriole Lake groves); column 2: SQF-complex [2020] affected Board Camp grove) (Figure S2). Models were checked graphically for convergence and the Rhat (\hat{r}) value was equal to 1. *See Methods: Statistical Analysis* for details.

Giant Sequoia
Diameter Breast Height ~ Crown Volume
Sillett et al. 2019 For. Ecol. Manag.

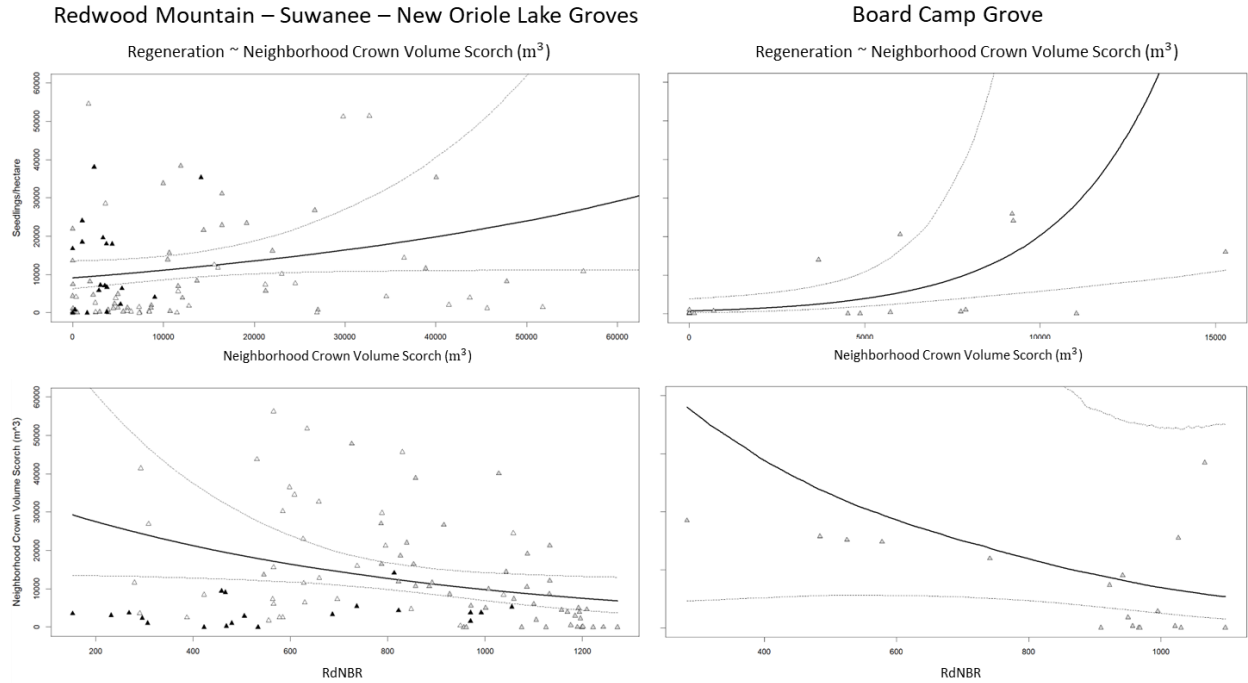


920

921 Figure S1. Modeled relationship between giant sequoia (*Sequoiadendron giganteum*) diameter at
922 breast height (cm) and crown volume (m³) based on data published in Sillett et al., 2019.

923

924



925

926 Figure S2. Visualizing the relationships between regeneration density (seedlings/hectare) and
 927 neighborhood crown volume scorch (top panel) and neighborhood crown volume scorch and
 928 RdNBR (bottom panel). Analyses are separated by groves that were affected by different
 929 fires/years (column 1: KNP-complex [2021] affected Redwood Mountain, Suwanee, and New
 930 Oriole Lake groves); column 2: SQF-complex [2020] affected Board Camp grove).